APPENDIX B

An Explicit Finite-Volume Time-Marching Procedure for Turbulent Flow Calculations

Stephen Nicholson, Joan G. Moore and John Moore

Mechanical Engineering Department
Virginia Polytechnic Institute and State University
Blacksburg, Virginia 24061

1. SUMMARY

A method has been developed which calculates two-dimensional, transonic, viscous flow in ducts. The finite-volume, time-marching formulation is used to obtain steady flow solutions of the Reynolds-averaged form of the Navier Stokes equations. The entire calculation is performed in the physical domain.

The features of the current method can be summarized as follows. Control volumes are chosen so that smoothing of flow properties, typically required for stability, is not needed. Different time steps are used in the different governing equations. A new pressure interpolation scheme is introduced which improves the shock capturing ability of the method. A multi-volume method for pressure changes in the boundary layer allows calculations which use very long and thin control volumes (length/height - 1000). The method is then compared here with two test cases. Essentially incompressible turbulent boundary layer flow in an adverse pressure gradient is calculated and the computed distributions of mean velocity and shear stress are in good agreement with the measurements. Transonic viscous flow in a converging diverging nozzle is calculated; the Mach number upstream of the shock is approximately 1.25. The agreement between the calculated and measured shock strength and total pressure losses is good.

2. INTRODUCTION

The finite volume method has been used extensively to solve the Euler equations for transonic flow including flow at high Mach numbers. In internal aerodynamics, McDonald [1] was the first investigator to use the time marching finite volume method. Denton [2] extended McDonald's finite-volume

method to three dimensions. Versions of Denton's method have been used in inviscid-viscous interaction programs for turbomachinery calculations [3-5].

The scope of the present work was to extend a finite volume method like that of Denton's to be able to calculate laminar or turbulent flow in ducts. The new method has the capability to calculate subsonic as well as transonic flow.

3. GOVERNING EQUATIONS

The unsteady form of the continuity equation, the x-momentum equation, and the y-momentum equation, in integral form, are used to obtain a steady-state solution for flow through 2-dimensional ducts. The ideal gas equation of state, the assumption of constant total temperature, and a Prandtl mixing length turbulence model complete the governing equations needed to solve for the unknown variables ρ, u, v, P, μ, and T.

For a finite control volume where we can assign one value of density to the control volume, and for a finite time step, δt, continuity states that,

$$\rho^{n+1} - \rho^{n} = \delta\rho = -\left[\iint \rho \underline{u} \cdot \underline{dA}\right] \frac{\delta t}{\delta Vol} \qquad (1)$$

where the integral is evaluated explicitly at the current time step, n. In arriving at an expression which relates the pressure change directly to the continuity error, we will assume that changes in temperature are small in comparison to other changes for one time step. Thus, we can relate changes in pressure to changes in density through the ideal gas equation of state,

$$P^{n+1} - P^{n} = \delta P = -RT\left[\iint \rho \underline{u} \cdot \underline{dA}\right] \frac{\delta t}{\delta Vol} \qquad (2)$$

For the method introduced in the current work, a non-conservative form of the unsteady momentum equation is used. The non-conservative form is used because it allows the use of different time steps for the continuity and momentum equations. The differences between the non-conservative and conservative forms of the unsteady momentum equations are associated with the unsteady and convective terms. Specifically, we note that

$$\frac{\partial(\rho \underline{u})}{\partial t} + \nabla \cdot \rho \underline{u}\,\underline{u} = \rho \frac{\partial \underline{u}}{\partial t} + \rho \underline{u} \cdot \nabla \underline{u} \qquad (3)$$

and the right hand side of Eq. (3) can be rewritten as

$$\rho \frac{\partial \underline{u}}{\partial t} + \rho \underline{u} \cdot \nabla \underline{u} = \rho \frac{\partial \underline{u}}{\partial t} + \nabla \cdot \rho \underline{u}\,\underline{u} - \underline{u}(\nabla \cdot \rho \underline{u}) \qquad (4)$$

When the right hand side of Eq. (4) is combined with the pressure and viscous terms, the momentum equation in integral form becomes

$$(\underline{u})^{n+1} - (\underline{u})^{n} = \delta(\underline{u}) = \left[-\iint \rho \underline{u}\,\underline{u} \cdot d\underline{A} + \bar{u} \iint \rho \underline{u} \cdot d\underline{A}\right.$$

$$\left. -\iint P\,\delta_{ij} \cdot d\underline{A} + \iint \left(\mu \nabla \underline{u} + \mu \overline{\nabla \underline{u}^{T}} \cdot d\underline{A}\right)\right] \frac{\delta t}{\delta Vol} \qquad (5)$$

To maintain stability, the properties must be updated in the proper sequence. In the current method, the sequence is

1. update the pressure from the continuity equation;
2. update the velocities from the momentum equation using the new pressure and old velocities and old density;
3. update the density from the ideal gas equation of state;
4. update the temperature from constant total temperature.

4. CONTROL VOLUMES

A new control volume has been introduced for this method. To eliminate the need for smoothing of flow properties, there must be as many control volumes across the duct as there are nodes where these variables are calculated. We need as many equations as unknowns. The control volumes also need to be located so that errors in continuity and momentum can correctly influence the changes in pressure or density and velocity without smoothing. The current control volume accomplishes this and is shown in Fig. 1. When calculating the flux through a streamwise face of an element, the value of the flow properties at the node on that face are used. Linear interpolation is used to obtain the flux on the cross-stream face.

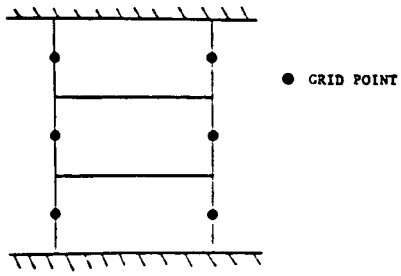

Fig. 1 New Control Volumes

5. DISTRIBUTION OF PROPERTIES

The properties at node points are changed in the flow field after each time step because the continuity and momentum equations are not satisfied for a given control volume. A decision must be made about which node, either upstream or downstream, these changes should be allocated to. The criterion used in determining where changes in properties should be sent is that these distributions result in reduced errors in continuity and momentum. The current method uses the following allocation procedure:

1. The pressure is updated through the continuity equation and the pressure change is sent to the upstream node;
2. The u and v velocities are updated through the momentum equations and the changes are sent to the downstream node;
3. The density is updated through the ideal gas equation of state using an interpolated pressure.

6. PRESSURE INTERPOLATION PROCEDURE

As part of the updating procedure used by Denton [5], an effective pressure is used in the momentum equations rather than the true thermodynamic pressure determined from the ideal gas equation of state. This effective pressure is needed because if the true pressure is used in the momentum equations the solution may not converge. In the current method, the density used in the continuity and momentum equations is an effective density which may be different than the density obtained using the ideal gas equation of state. This effective density is used to satisfy stability requirements.

Starting with a generalized pressure interpolation equation for the effective density

$$\rho_{I+1} = \left[P_I + a_0(P_{I+1} - P_I) + a_1 \frac{(P_{I+1} - P_{I-1})}{2} + a_2 \frac{(P_{I+1} - P_{I-2})}{3}\right] \frac{1}{RT_{I+1}} , \qquad (6)$$

Mach number limitations were sought for a_0, a_1, and a_2 such that

$$a_1 + a_2 + a_3 = 1 \qquad (7)$$

which assures second order accurate solutions. A set of equations for a_0, a_1, and a_2 was chosen which satisfies two stability criteria [6]. The equations are

for $M < 2$ $\quad a_0 = \left(\frac{0.8}{3}\right)\left(\frac{4}{M^2} - 1\right)$; $a_1 = 1 - a_0$; $a_2 = 0$:

for $M > 2$ $\quad a_0 = 0$; $a_1 = 4/M^2$; $a_2 = 1 - a_1$. (8)

These Mach number dependent formulations for a_0, a_1, and a_2 are shown in Fig. 2.

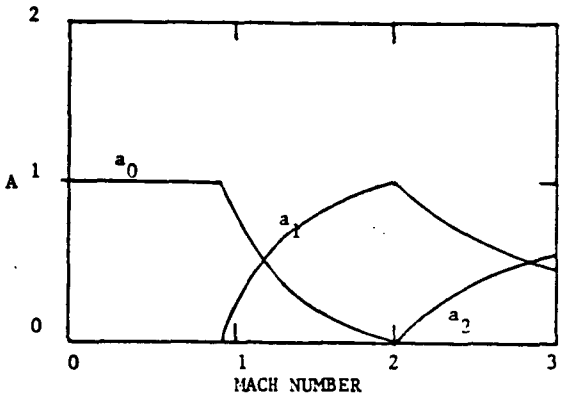

Fig. 2 Mach Number Dependent Values for Coefficients a_0, a_1, and a_2

7. TIME STEPS

A unique feature of this method is the use of different time steps for the continuity and momentum equations. Previous workers who have used explicit time marching methods have used the CFL condition as a basis for determining allowable time steps which maintain stability. The same time step is used for both the continuity and momentum equations. In the current method, the expressions that are used to determine the allowable time steps are; for the momentum equations

$$\delta t_m < \frac{1}{\left|\frac{u}{\delta x}\right| + \left|\frac{v_{eff}}{\delta y}\right| + \left|\frac{2\mu}{\rho(\delta y)^2}\right|} \tag{9}$$

and for continuity,

$$\delta t_c < \frac{1}{2RT\left[\frac{\delta t_m}{(\delta x)^2} + \frac{\delta t_m}{(\delta y)^2} + \left|\frac{u}{RT\delta x}\right| + \left|\frac{v}{RT\delta y}\right|\right]} \tag{10}$$

where δt_m is the momentum time step, δt_c is the continuity time step and v_{eff} is an effective y-component of velocity. The advantage of using different time steps is that, for low

velocity regions of the flow, the allowable momentum time step can be significantly larger than that allowed by the CFL condition. These larger time steps allow the boundary layer profiles to change more rapidly and enhance the convergence rate significantly compared with a method which uses the CFL condition.

8. BOUNDARY CONDITIONS

For viscous flow, at the upstream boundary, the total temperature, freestream total pressure, inlet boundary layer velocity profile, and flow angle are specified. Along the downstream boundary the static pressure is specified. Pressures along the solid boundaries are determined from linear extrapolation. For viscous flow, the values of the x-component and y-component of velocity are set equal to zero at solid walls.

9. TURBULENCE MODEL

A Prandtl mixing length model is used to model the turbulent stresses. The model is

$$\mu_{eff} = \mu_\ell + \mu_t \qquad \mu_t = \rho L^2 \left|\frac{du}{dy}\right|$$

L is smaller of 0.08 times the width of boundary layer
or 0.41 times the distance to the wall

Van Driest Correction

$$L = 0.41\,|y|\left(1 - \exp\left[-|y|\sqrt{\rho\tau}/26\,\mu_\ell\right]\right)$$

Near Wall Correction $\quad \mu_{eff} = \sqrt{\mu_\ell(\mu_\ell + \mu_t)}$

10. MULTI-VOLUME METHOD FOR PRESSURE CHANGES

Control volumes are grouped in the boundary layer to form a larger global control volume. The continuity error is calculated for this global control volume and changes in pressure are assigned equally to each of the upstream nodes for each control volume making up the global control volume. Then the global control volume is made successively smaller towards the wall. This is shown schematically in Fig. 3. The entire pressure change for one iteration at each node within the multi-volume region is determined by adding together all the pressure changes assigned to that node.

The multi-volume method propagates pressure changes rapidly through the boundary layer and minimizes transverse pressure gradients in the intermediate solution. The above changes allow the calculation of boundary layer flows where

the control volumes near the wall can have aspect ratios (length/height) over 1000.

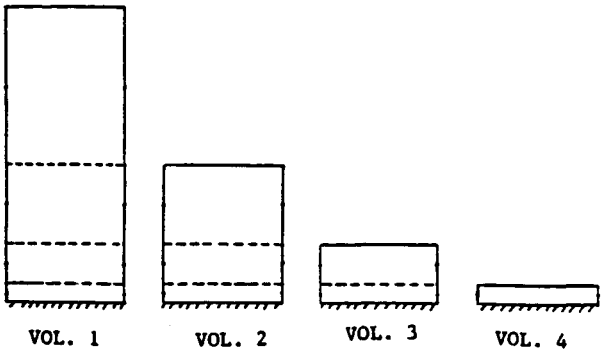

Fig. 3 Multi-Volume Method for Pressure Changes in the Boundary Layer

11. TRANSVERSE UPWIND DIFFERENCING

When the control volumes become long and thin near the wall of the duct, the fluxes through the top and bottom faces of the control volume become more significant in comparison to the fluxes through the streamwise faces. To strengthen the diagonal dominance of the coefficient matrix, the momentum fluxes through the transverse faces may be calculated using interpolated velocities upstream in the transverse direction rather than the actual interpolated values. The interpolation functions and the derivation of the functions is discussed in more detail in Ref. 6.

12. SAMUEL AND JOUBERT INCOMPRESSIBLE TURBULENT BOUNDARY LAYER

Incompressible turbulent boundary layer flow in a diverging duct was calculated for test case 0141 of the Stanford Conference [7]. The grid used in the present calculations is shown in Fig. 4. The inlet velocity is 26 m/s.

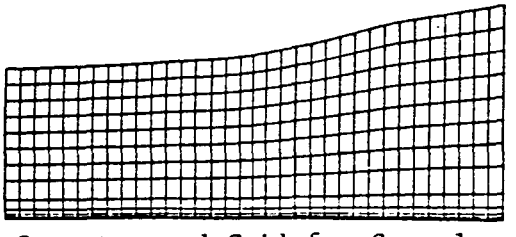

Fig. 4 Geometry and Grid for Samuel and Joubert

Figure 5a shows a comparison of the calculated skin friction coefficient with the experimental results and with the results from the Moore cascade flow program. The agreement is excellent. A comparison of the calculated turbulent shear stress distribution, $\overline{uv}$, with the experi-

mental results is shown in Fig. 5b. The agreement is good. Figure 5c shows good agreement also between the calculated and measured velocity profiles at two locations in the duct.

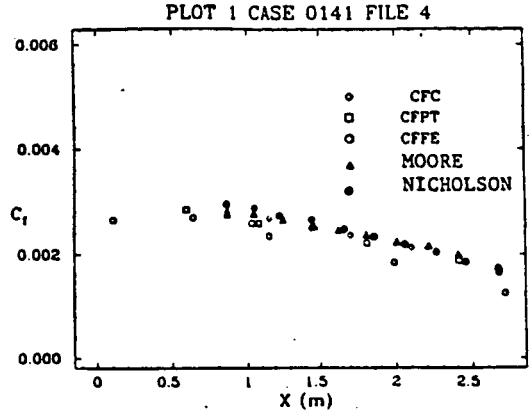

5a) Skin Friction Coefficient

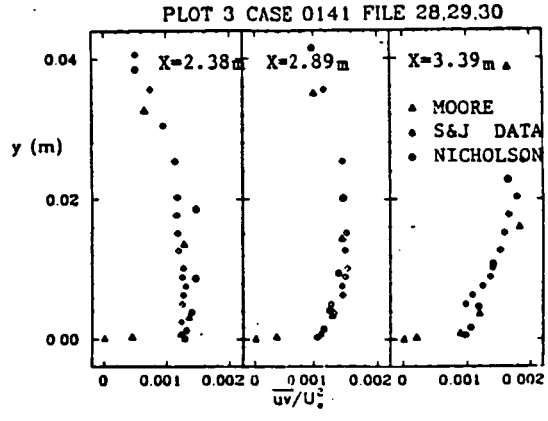

5b) Turbulent Shear Stresses

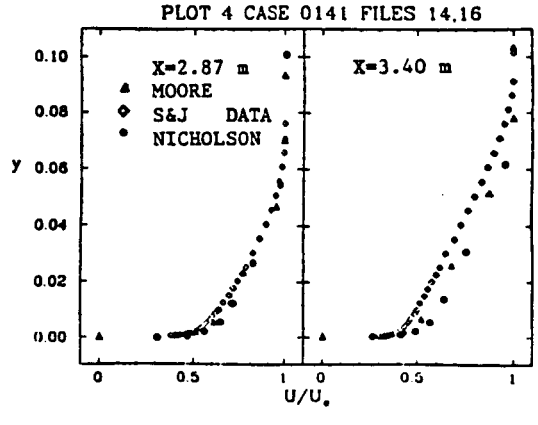

5c) Velocity Profiles

Fig. 5 Results for Samuel and Joubert

13. MDRL DIFFUSER CALCULATIONS

The diffuser geometry (Model G) is shown in Figure 6a [8,9]. Figure 6a also shows the computational grid used which has 87 grid points in the axial direction and 20 points across the flow. The inlet boundary layer thicknesses were specified as 9% and 4.5% of the inlet diffuser height for the curved and flat wall boundary layers, respectively. For this calculation, the ratio of exit static pressure to the inlet total pressure was 0.826. In the experiment, this test point results in transonic flow in the diverging portion of the duct with a Mach number of approximately 1.235 upstream of a nearly normal shock, and the flow remained fully-attached throughout the diffuser at this test condition.

A contour plot of static pressure is shown in Fig. 6b. The shock can be seen in the diverging portion of the duct. The shock is well defined as illustrated by the high clustering of contours at the shock. Figure 6c shows a Mach number contour plot for the calculations. The calculated and measured curved wall static pressures are compared in Fig. 7. The shock is well defined and no overshoot occurs in the static pressure.

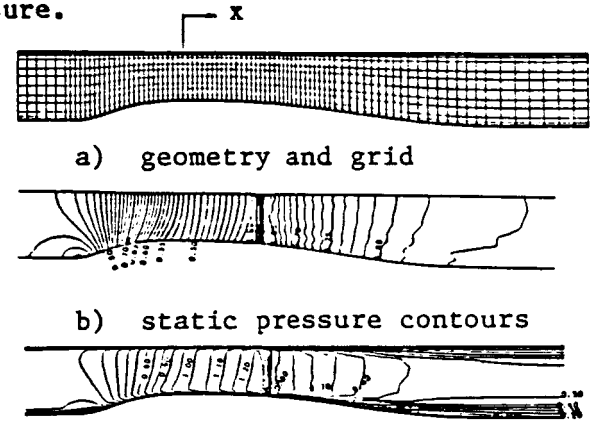

Fig. 6 Geometry and Contours for MDRL Diffuser

Measured shock locations on the curved wall and in the middle of the duct are plotted in Fig. 8 as a function of shock Mach number, $M_{\sigma u}$, determined from the minimum wall static pressures on the curved wall. The minimum wall static pressure in the calculation is located at x/h = 1.5; this is taken to be the location of the shock. The Mach number upstream of the shock was determined to be 1.256 from the calculated total pressure ratio across the shock in the freestream. This result is plotted in Fig. 8 and it agrees well with the measured shock location. Comparisons of calculated and measured velocity profiles (see Ref. 9) at two axial locations along the duct are shown in Fig. 9. The agreement is good. The mass averaged total pressure at the diffuser exit divided by the inlet freestream total pressure

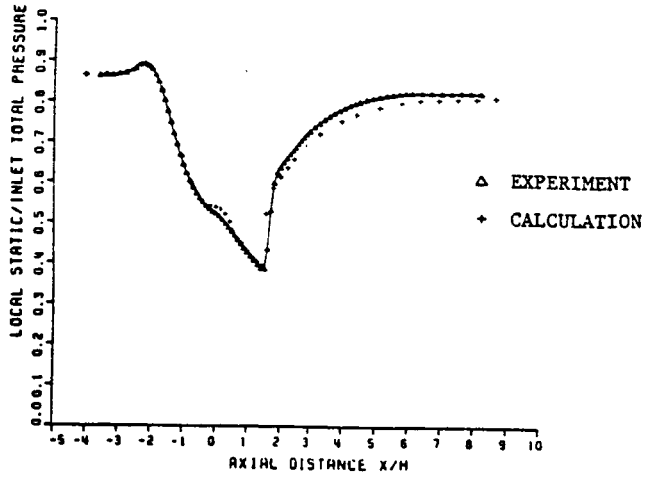

Fig. 7 Curved Wall Static Pressures for MDRL Diffuser

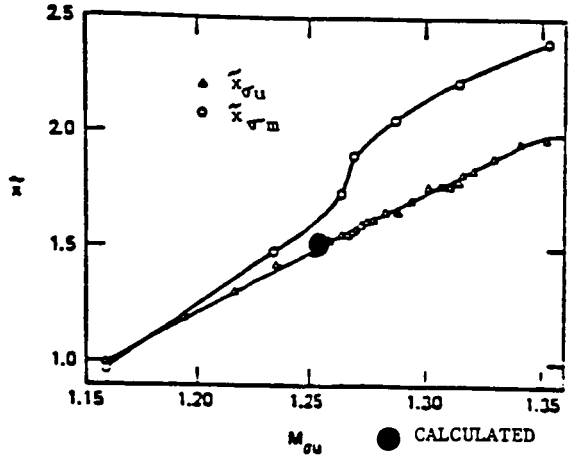

Fig. 8 Comparison of Computed and Measured Shock Position in MDRL Diffuser

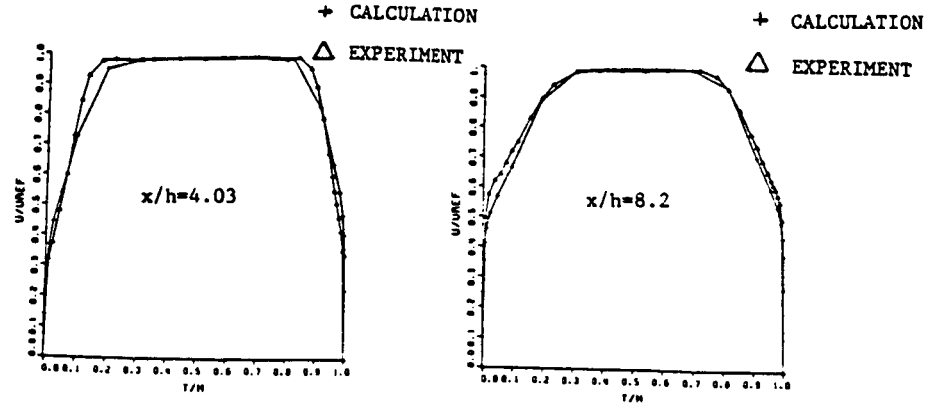

Fig. 9 Velocity Profiles at x/h= 4.03 and 8.2 in MDRL Diffuser

is calculated from the numerical results to be 0.9615. This compares well with the measured value of 0.965, obtained from the data of M. Sajben and T. J. Bogar, midway between the diffuser side walls.

The total CPU time for the MDRL diffuser calculations was approximately 35 minutes on an IBM 3031.

14. CONCLUSIONS

An explicit finite volume time marching method has been extended to allow the calculation of laminar and turbulent flow in ducts. Both subsonic and supersonic flow can be calculated with the method. Incompressible turbulent boundary layer flow in an adverse pressure gradient was calculated. The agreement between the calculated and measured skin friction coefficient, turbulent shear stress distribution, and mean velocity profiles was good. Transonic viscous flow through a converging diverging nozzle was calculated. The computed and measured velocity profiles were in good agreement especially near the exit of the nozzle. The computed and measured shock locations were compared and were found to be in good agreement. Viscous and shock losses in the diffuser were well modelled.

15. ACKNOWLEDGMENTS

This work was supported by NASA Lewis Research Center under NASA grant NAG 3-593. The authors are grateful to Jerry R. Wood and Lou A. Povinelli for their encouragement and technical assistance. Miklos Sajben and Thomas J. Bogar kindly provided data on their diffuser tests at the McDonnell Douglas Research Laboratories, in Saint Louis, Missouri.

16. REFERENCES

1. MCDONALD, P. W. - The Computation of Transonic Flow Through Two Dimensional Gas Turbine Cascades. ASME Paper 71-GT-89.
2. DENTON, J. D. - Extension of the Finite Area Time Marching Method to Three Dimensions. VKI Lecture Series 84, Transonic Flow in Axial Turbomachines, February 1976.
3. SINGH, U. K. - A Computation and Comparison with Measurement of Transonic Flow in an Axial Compressor with Shock and Boundary Layer Interaction. ASME Paper 81-Gr/GT-5.
4. CALVERT, W. J. - An Inviscid-Viscous Interaction Treatment to Predict the Blade-to-Blade Performance of Axial Compressors with Leading Edge Normal Shock Waves. ASME Paper 82-GT-135.

5. DENTON, J. D. - An Improved Time Marching Method for Turbomachinery Calculations. ASME Paper 82-GT-239.
6. NICHOLSON, S. - Extension of the Finite Volume Method to Laminar and Turbulent Flow. Ph.D. Thesis, Virginia Polytechnic Institute and State University, Blacksburg, VA, 1986.
7. KLINE, S. J., CANTWELL, B. J., and LILLEY, G. M. - Complex Turbulent Flow Computation-Experiment. 1980-81 AFOSR-HTTM-Stanford Conference on Complex Turbulent Flows, 1982.
8. BOGAR, T. J., SAJBEN, M., and KROUTIL, J. C. - Characteristic Frequency and Length Scale in Transonic Diffuser Flow Oscillations. AIAA Paper 81-1291.
9. SALMON, J. T., BOGAR, T. J., and SAJBEN, M. - Laser Velocimeter Measurements in Unsteady, Separated, Transonic Diffuser Flows. AIAA Paper 81-1197.